JOURNAL OF SOLID STATE CHEMISTRY **132,** 249–256 (1997)
ARTICLE NO. SC977416

A Sodium Molybdenyl Monophosphate with an Intersecting Tunnel Structure: $Na_3(MoO)_2(PO_4)_3$

S. Ledain, A. Leclaire, M. M. Borel, and B. Raveau

Laboratoire CRISMAT, UMR-6508 associé au CNRS, ISMRA et Université de Caen 6, Boulevard du Maréchal Juin, 14050 Caen Cedex, France

Received October 21, 1996; in revised form April 4, 1997; accepted April 8, 1997

A new sodium molybdenyl monophosphate $Na_3(MoO)_2(PO_4)_3$ has been synthesized. It crystallizes in the space group $C2/c$ with $a = 15.211(2)$ Å, $b = 8.909(1)$ Å, $c = 9.362(1)$ Å, and $\beta = 115°99(1)$. The $[Mo_2P_3O_{14}]_\infty$ three-dimensional framework can be described from isolated MoO_6 octahedra connected through monophosphate groups, forming $[Mo_2P_3O_{14}]_\infty$ ribbons running along b. The most stricking feature concerns the exceptional opened character of this structure. It exhibits large 10-sided tunnels running along c and interconnected through large octahedral windows; moreover the latter intersect with 6-sided tunnels running along [101] and [10$\bar{1}$]. The distribution of the sodium cations in these tunnels and their coordination are described; their high thermal factors up to 7 Å^2 suggest a possibility of ionic mobility. A comparison with the other sodium Mo(V) phosphates known to date is presented. © 1997 Academic Press

INTRODUCTION

The research of structures with an opened framework containing sodium cations has been and remains of high interest for the realization of cationic exchanges and of ionic superconductors. Besides the famous β Alumina, and Nasicon, phosphates of pentavalent molybdenum containing sodium can be considered as potential materials due to the particular electronic configuration of Mo(V). The latter exhibits indeed an octahedral coordination, but is off-centered in its MoO_6 octahedron, forming one abnormally short Mo–O bond, so that the corresponding oxygen apex is systematically free. As a result, the "MoPO" framework is made more flexible, allowing tunnel and cage structures to be synthesized.

Numerous Mo(V) phosphates have been discovered these past 10 years (see for a review Refs. 1, 2), but among them, only four compounds are pure sodium anhydra phosphates, the monophosphate $Na(MoO)_4(PO_4)_5$ (3), the diphosphate $NaMoOP_2O_7$ (4), and the two forms of phosphates ε- and ζ-$Na(MoO)_2P_2O_7(PO_4)$ (5, 6). Moreover, the sodium content in these phases is rather low. Attempts to increase this content in order to enhance the opened character of the structure were undertaken. In this respect, the monophosphate $Li_2Na(MoO)_2(PO_4)_3$ (7) is of interest since it shows the possibility of increasing alkaline cation content to stabilize an intersecting tunnel structure. Nevertheless, due to the small size of lithium, the tunnels where these cations are located are not favorable for a high cationic mobility. For this reason we have investigated the possibility of synthesizing a similar structure but containing only sodium. In the present paper, we report on a new Mo(V) monophosphate $Na_3(MoO)_2(PO_4)_3$ which exhibits an original three-dimensional framework, forming large intersecting tunnels, and we discuss the crystal chemistry of the sodium molybdenyl phosphates.

EXPERIMENTAL SECTION

Chemical Synthesis and Crystal Growth

Attempts to prepare a phase with composition $Na_3(MoO)_2(PO_4)_3$ were carried out in two steps. First an intimate mixture of MoO_3, $H(NH_4)_2PO_4$, and Na_2CO_3 in the molar ratio 3.33 : 6 : 3 was heated in air up to 400°C in a platinum crucible to eliminate CO_2, NH_3, and H_2O. Then the appropriate amount of molybdenum was added and the finely ground mixture was sealed in a silica ampoule. The latter was heated for 24 h at varying temperature ranging from 570 to 630°C and cooled down to room temperature at a rate of 3.3°C h^{-1}. Whatever the temperature, we obtained a polycrystalline sample that was biphasic. The major phase (about 90%), which consists of green microcrystals, was identified from the chemical analysis as $Na_3Mo_2P_3O_{14}$, whereas the minor phase which is brown has not yet been identified.

Single crystals of this new phosphate were then grown from a mixture of nominal composition $NaMoPO_5$. The first step which deals with decarbonation and dehydration is similar to that described above for the synthesis. In the second step, a similar experimental method is used, except that the mixture is heated at 630°C for 24 h, cooled down to 550°C at a speed of 3.3°Ch^{-1}, and finally quenched to room temperature.

0022-4596/97 $25.00

Energy Dispersive Analysis (EDS)

The elementary analysis of the elements Na, Mo, P was performed with a Tracor microprobe mounted on a scanning electron microscope; it allowed the "$Na_3Mo_2P_3$" composition to be established in agreement with the structure determination.

X-ray Diffraction Study

Different crystals were tested by the precession and Weissenberg methods using Cu$K\alpha$ radiation.

A yellow green crystal with dimensions $0.045 \times 0.064 \times 0.013$ mm was selected for the structure determination. The cell parameters were determined by diffractometric techniques at 25°C with a least-squares refinement based upon 25 reflections with $18° < \theta < 22°$. The data were collected on a CAD4 Enraf-Nonius diffractometer with the parameters reported in Table 1. The systematic extinctions $h + k = 2n + 1$ for hkl and $l = 2n + 1$ for $h0l$ are consistent with the space group $C2/c$ or Cc. The reflections were corrected for Lorentzian and polarization effects and for absorption. The structure was solved with a heavy atom method and the Harker peaks show that the space group is $C2/c$.

The refinement of the atomic coordinates, their anisotropic thermal parameters for Mo, P, O, and Na, and the population of the sodium atoms led to $R = 0.036$ and $R_w = 0.029$ and to the atomic parameters of Table 2.

TABLE 1
Summary of Crystal Data, Intensity Measurements, and Structure Refinement Parameters for $Na_3(MoO)_2(PO_4)_3$

1. Crystal data	
Space group	$C2/c$
Cell dimensions	$a = 15.211(2)$ Å
	$b = 8.9093(8)$ Å, $\beta = 115.99(1)°$
	$c = 9.362(1)$ Å
Volume (Å)^3	1140.6(2) Å^3
Z	8
ρ_{calc} (gcm^3)	3.365
2. Intensity measurements	
λ(Mo$K\alpha$)	0.71073
Scan mode	$\omega - \theta$
Scan width (°)	$1.0 + 0.35 \tan\theta$
Slit aperture (mm)	$1.0 + \tan\theta$
Max θ(°)	45
Standard reflections	3 measured every 3600 s
Measured reflections	4849
Reflections with $I > 3\sigma$	759
μ (mm^{-1})	2.82
3. Structure solution and refinement	
Parameters refined	127
Agreement factors	$R = 0.036$, $R_w = 0.029$
Weighting scheme	$w = 1/\sigma^2$
Δ/σ max	< 0.005

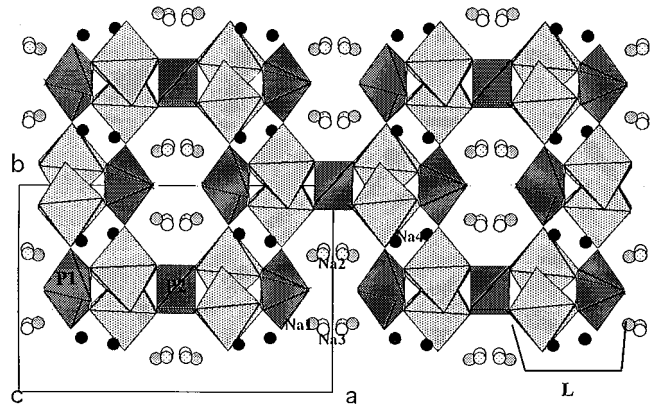

FIG. 1. Projection of the structure of $Na_3(MoO)_2(PO_4)_3$ along **c**.

RESULTS AND DISCUSSION

Description of the $[Mo_2P_3O_{14}]_\infty$ Host Lattice

The projection of this structure along **c** (Fig. 1) shows the highly opened character of the $[Mo_2P_3O_{14}]_\infty$ framework. One indeed observes large 10-sided tunnels running along **c** that are formed from four MoO_6 octahedra and six PO_4 tetrahedra sharing their apices.

In fact the three-dimensional $[Mo_2P_3O_{14}]_\infty$ framework can be simply described by considering its projection along **b** (Fig. 2). It shows that it consists of single monophosphate groups sharing their four apices with isolated MoO_6 octahedra. But the most striking feature deals with the fact that the whole framework is formed by the stacking of

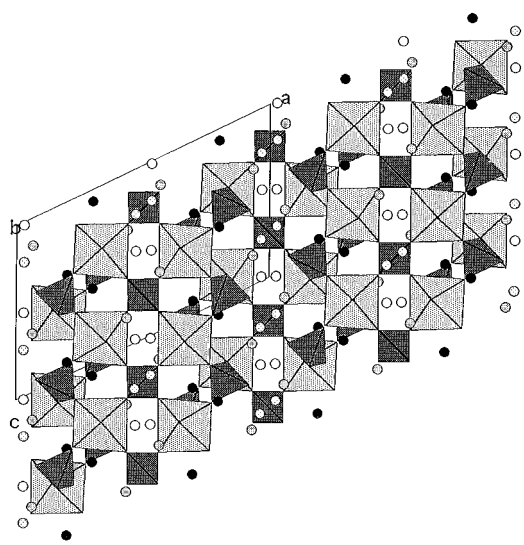

FIG. 2. Projection of the structure of $Na_3(MoO)_2(PO_4)_3$ along **b**.

TABLE 2
Positional Parameters and Their Estimated Standard Deviations in $Na_3(MoO)_2(PO_4)_3$

Atom	x	y	z	B (Å^2)	Population
Mo	0.16593(6)	0.0696(1)	0.1178(1)	0.80(2)	1.0
P(1)	0.1715(2)	0.4415(3)	0.0380(3)	0.90(6)	1.0
P(2)	0.0	− 0.0121(4)	0.25	0.80(8)	1.0
Na(1)	0.4358(5)	0.1627(9)	0.337(1)	3.1(3)	0.71(2)
Na(2)	− 0.0310(9)	0.331(1)	0.267(2)	4.5(6)	0.42(1)
Na(3)	− 0.030(2)	0.308(2)	− 0.019(7)	7(2)	0.25(2)
Na(4)	0.200(2)	0.267(4)	0.426(4)	3(2)	0.14(1)
O(1)	0.1448(5)	− 0.1147(7)	0.0846(8)	1.9(2)	1.0
O(2)	0.2681(4)	0.0645(8)	0.3419(7)	1.8(2)	1.0
O(3)	0.0609(5)	0.0936(8)	0.2013(8)	1.8(2)	1.0
O(4)	0.2760(5)	0.1017(8)	0.0630(9)	2.4(3)	1.0
O(5)	0.0624(5)	0.1176(6)	− 0.1143(7)	1.4(2)	1.0
O(6)	0.1646(6)	0.3040(6)	0.1323(8)	1.3(2)	1.0
O(7)	0.0727(4)	0.5030(8)	− 0.0679(9)	2.3(2)	1.0

Atomic Displacement Parameters

	U_{11}	U_{22}	U_{33}	U_{12}	U_{13}	U_{23}
Mo(1)	0.0124(4)	0.0082(3)	0.0089(3)	− 0.0017(5)	0.0041(3)	− 0.0004(6)
P(1)	0.011(1)	0.011(1)	0.013(1)	− 0.001(1)	0.0060(9)	− 0.001(1)
P(2)	0.007(2)	0.011(2)	0.012(2)	0	0.005(1)	0
O(1)	0.026(4)	0.011(3)	0.026(4)	− 0.005(3)	0.004(4)	− 0.002(3)
O(2)	0.032(4)	0.010(3)	0.015(3)	0.005(4)	0.000(3)	0.006(4)
O(3)	0.021(4)	0.019(4)	0.035(4)	− 0.009(3)	0.021(3)	0.001(3)
O(4)	0.041(5)	0.022(5)	0.048(5)	− 0.005(3)	0.037(4)	− 0.006(4)
O(5)	0.023(4)	0.010(3)	0.010(3)	0.001(3)	− 0.000(3)	0.005(3)
O(6)	0.029(4)	0.012(3)	0.009(3)	− 0.004(3)	0.010(3)	0.003(3)
O(7)	0.007(3)	0.031(4)	0.035(4)	0.002(3)	− 0.004(3)	0.009(3)
Na(1)	0.038(5)	0.022(4)	0.053(6)	− 0.001(3)	0.016(4)	0.008(4)
Na(2)	0.06(1)	0.014(5)	0.05(1)	− 0.018(5)	− 0.013(9)	0.009(7)
Na(3)	0.07(2)	0.04(1)	0.21(6)	0.02(1)	0.11(3)	0.04(2)
Na(4)	0.05(2)	0.04(2)	0.03(2)	0.02(2)	0.03(2)	0.00(2)

Note. Anisotropically refined atoms are given in the form of the isotropic equivalent displacement parameter defined as $B = \frac{4}{3}\sum_i \sum_j \mathbf{a}_i \mathbf{a}_j \beta_{ij}$.

$[Mo_2P_3O_{16}]_\infty$ ribbons running along **c**. The projection of such a ribbon along **b**, whose mean plane is parallel to (010), is shown in Fig. 3. It consists of two rows of Mo octahedra interconnected through one row of P(2) tetrahedra and bordered by two rows of P(1) tetrahedra. Note that at a similar y level ($y = 0.0696$ or 0.5696) those ribbons are disconnected from one another. Consequently, in each ribbon the Mo octahedron shares its four basal apices with four PO_4 tetrahedra (2 P(1) + 2 P(2)), whereas each P(2) tetrahedron is linked to four Mo octahedra, and each P(1) tatrahedron shares two apices with two Mo octahedra. Then, two adjacent $[Mo_2P_3O_{16}]_\infty$ ribbons located at two different levels along **b** (Fig. 2) are connected to each other through their P(1) tetrahedra and Mo octahedra respectively. Each P(1) tetrahedron of one $[Mo_2P_3O_{16}]_\infty$ ribbon shares one apex with one Mo octahedron of the ribbon located either above or below it. It results that each P(1) tetrahedron exhibits one free apex directed toward the center of the 10-sided tunnels, and that similarly for each Mo octahedron with respect to the $[Mo_2P_3O_{16}]_\infty$ ribbon.

The consideration of the layers of polyhedra parallel to (100) (labeled L in Fig. 1) which form the walls of the 10-sided tunnels is of great interest. The projection of such a $[Mo_2P_2O_{14}]_\infty$ layer onto (100) (Fig. 4) shows that it consists of $[MoPO_8]_\infty$ chains running along **c** and along **b**. These types of chains where one MoO_6 octahedron alternates with one PO_4 tetrahedron are currently observed in molybdenum phosphates. But, most important is the fact that two successive enantiomorphic $[MoPO_8]_\infty$ chains parallel to **b** form large octagonal windows built up of four octahedra and four tetrahedra. The smallest dimension of this window (distance between two opposite oxygen atoms) is about 4.8 Å, allowing the mobility of ions with size less than 2 Å. The large 10-sided tunnels, the smallest dimension of which is about 5.9 Å, are interconnected through these windows.

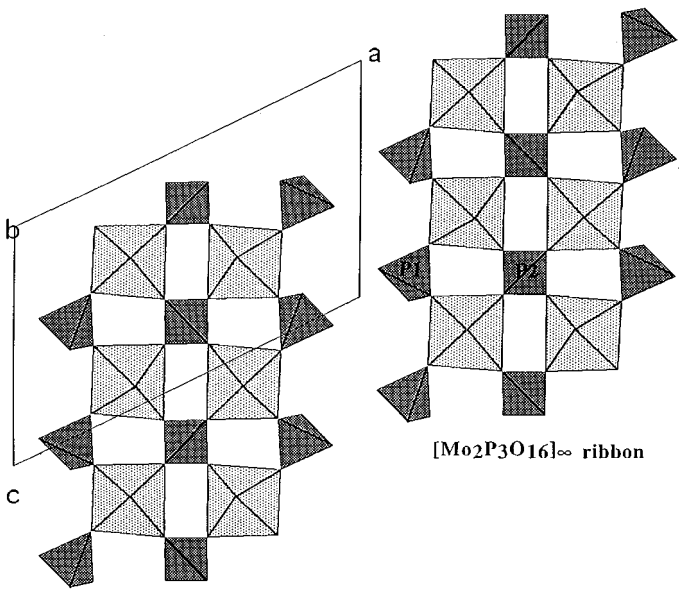

FIG. 3. Projection of a $[Mo_2P_3O_{16}]_\infty$ ribbon along **b**.

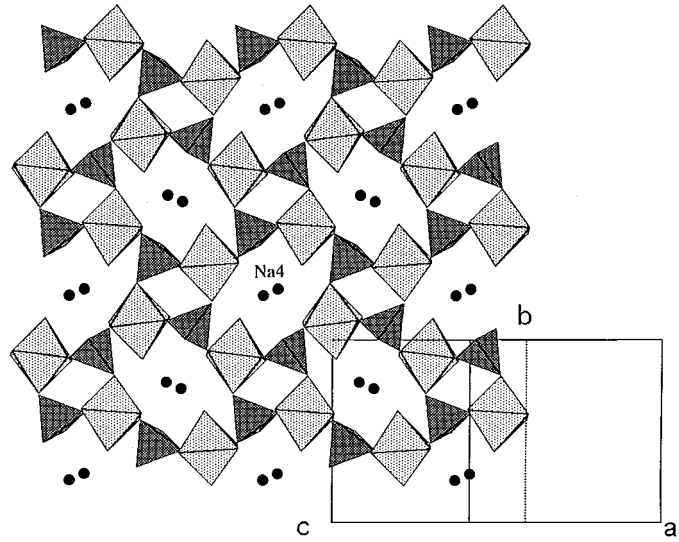

FIG. 4. Projection of a $[Mo_2P_3O_{14}]_\infty$ layer onto (100).

The projections of the $[Mo_2P_3O_{14}]_\infty$ framework along [101] (Fig. 5) and $[10\bar{1}]$ (Fig. 6) are also remarkable. They show the existence of six-sided tunnels running along the [101] and $[10\bar{1}]$ directions respectively. Thus the framework $[Mo_2P_3O_{14}]_\infty$ must be considered as exceptionally opened due to the large size of its tunnels, to their interconnection through lateral windows, and to the intersecting nature of the [001], [101], and $[10\bar{1}]$ tunnels.

The geometry of the MoO_6 octahedron (Table 3) is characteristic of Mo(V) with an abnormally short Mo–O bond (1.676 Å) corresponding to the free apex, opposite a longer bond (2.093 Å) with four intermediate bonds ranging from 1.991 to 2.094 Å.

The PO_4 tetrahedra exhibit P–O rather regular bonds (1.525 to 1.540 Å) except for the P(1)–O(7) bond (1.495 Å) corresponding to the free apex of the P(1) tetrahedron.

The Pentavalent Character of Molybdenum

In order to check the valence of molybdenum, electrostatic valence distribution has been calculated with the Brese and O'Keeffe procedure, but using a more appropriate

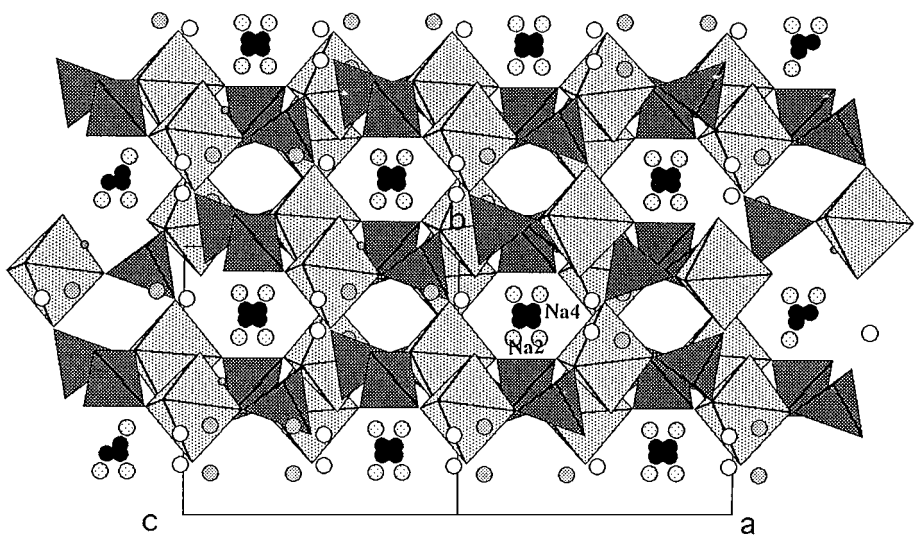

FIG. 5. Projection of the $[Mo_2P_3O_{14}]_\infty$ framework along [101].

TABLE 3
Distances (Å) and Angles (°) in the Polyhedra in $Na_3(MoO)_2(PO_4)_3$

Mo	O(1)	O(2)	O(3)	O(4)	O(5)	O(6)
O(1)	**1.676(6)**	2.812(8)	2.74(1)	2.85(1)	2.697(8)	3.753(8)
O(2)	99.8(3)	**1.991(5)**	2.845(9)	2.69(1)	4.067(1)	2.859(9)
O(3)	93.1(4)	88.8(3)	**2.075(9)**	4.013(1)	2.97(1)	2.70(1)
O(4)	102.1(4)	85.3(3)	164.5(3)	**1.97(1)**	2.933(9)	2.74(1)
O(5)	90.7(3)	169.5(3)	91.0(3)	92.2(3)	**2.094(5)**	2.713(8)
O(6)	169.4(3)	88.8(3)	80.9(3)	84.6(3)	80.8(2)	**2.093(6)**

P(1)	O(6)	$O(7)^{i}$	$O(2)^{i}$	O(4)
O(6)	**1.540(8)**	2.513(9)	2.51(1)	2.51(1)
$O(7)^{i}$	111.7(5)	**1.495(6)**	2.480(8)	2.47(1)
$O(2)^{i}$	108.3(4)	109.0(4)	**1.551(7)**	2.50(1)
O(4)	109.8(5)	109.1(4)	108.8(4)	**1.53(1)**

P(2)	O(3)	$O(3)^{ii}$	$O(5)^{iii}$	$O(5)^{iv}$
O(3)	**1.525(8)**	2.40(1)	2.526(9)	2.55(1)
$O(3)^{ii}$	103.6(5)	**1.525(8)**	2.55(1)	2.526(9)
$O(5)^{iii}$	111.6(4)	113.0(3)	**1.530(6)**	2.415(7)
$O(5)^{iv}$	113.0(3)	111.6(4)	104.3(4)	**1.530(6)**

Na(1)–O(1)^{v}: 2.60(1)
Na(1)–O(2): 2.72(1)
Na(1)–O(4): 2.71(1)
Na(1)–O(5)^{i}: 2.64(1)
Na(1)–O(5)^{vi}: 2.87(1)
Na(1)–O(7)^{i}: 2.88(1)
Na(1)–O(7)^{vi}: 2.64(1)
Na(1)–O(7)^{vii}: 2.38(1)

Na(2)–O(3): 2.75(2)
Na(2)–O(3)^{ii}: 2.21(1)
Na(2)–O(6)^{ii}: 2.60(2)
Na(2)–O(7)^{viii}: 2.24(2)
Na(2)–O(7)^{iv}: 2.22(1)

Na(3)–O(1): 2.33(3)
Na(3)–O(2)^{viii}: 2.98(3)
Na(3)–O(3): 2.70(4)
Na(3)–O(5): 2.60(5)
Na(3)–O(6): 2.67(3)
Na(3)–O(7): 2.51(4)
Na(3)–O(7)^{viii}: 2.09(4)

Na(4)–O(1)^{iv}: 2.42(4)
Na(4)–O(1)^{v}: 2.62(4)
Na(4)–O(2)^{i}: 2.51(4)
Na(4)–O(2): 2.37(4)
Na(4)–O(3): 2.72(3)
Na(4)–O(4): 3.00(4)
Na(4)–O(6): 2.58(4)
Na(4)–O(7)^{iv}: 2.37(4)

Symmetry codes
i: $-x-\frac{3}{2}; -y-\frac{3}{2}; -z$
ii: $-x; y; \frac{1}{2}-z$
iii: $-x; -y; -z$
iv: $x; -y; -\frac{3}{2}+z$
v: $-x+\frac{1}{2}; y+\frac{1}{2}; -z+\frac{1}{2}$
vi: $x-\frac{3}{2}; -y-\frac{3}{2}; z-\frac{3}{2}$
vii: $-x+\frac{1}{2}; y-\frac{1}{2}; -z+\frac{1}{2}$
viii: $-x; -y-1; -z$
ix: $-\frac{1}{2}+x; -y-\frac{3}{2}; z-\frac{1}{2}$

Note. The Mo–O or P–O distances are on the diagonal, the O···O distances are above it, and the O–Mo–O or O–P–O angles are below it.

R_{ij} value proposed by Leclaire *et al.* (3). These results, listed in Table 4, are in agreement with the value V for molybdenum and phosphorus, and I for sodium, and II for oxygen.

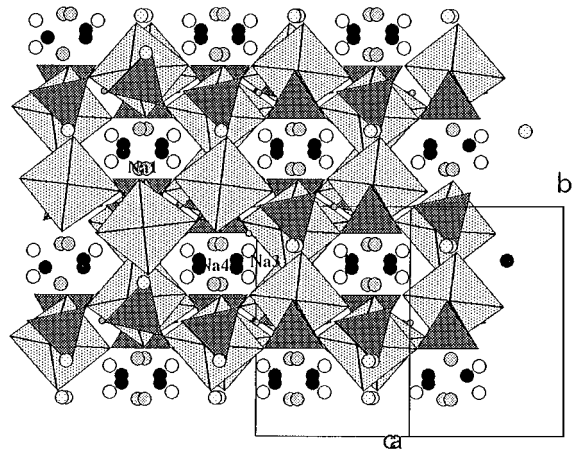

FIG. 6. Projection of the $[Mo_2P_3O_{16}]_\infty$ framework along $[10\bar{1}]$.

The Distribution and Coordination of Sodium

The sodium cations are distributed over four different sites. It is remarkable that all these sites are partly occupied

TABLE 4
Electrostatic Valence Distribution for $Na_3(MoO)_2(PO_4)_3$

	Mo	P(1)	P(2)	Na(1)	Na(2)	Na(3)	Na(4)	$\sum vi^-$
O(1)	1.747			0.082		0.060	0.015	**1.930**
							0.026	
				0.033		0.179	0.094	
							0.161	
O(2)	0.746	1.154		0.059		0.010	0.020	**2.019**
							0.030	
				0.024		0.031	0.127	
							0.184	
O(3)	0.594		1.238 × 2		0.032	0.022	0.012	**2.040**
					0.138			
					0.044	0.066	0.071	
					0.192			
O(4)	0.789	1.221		0.060			0.005	**2.075**
				0.025			0.034	
O(5)	0.564		1.221 × 2	0.073	0.029			**1.926**
					0.039			
				0.030	0.086			
				0.016				
O(6)	0.566	1.189			0.048	0.024	0.017	**1.844**
					0.067	0.071	0.104	
O(7)		1.342		0.038	0.126	0.037	0.008	**2.020**
				0.073	0.135	0.114		
				0.149				
				0.016	0.174	0.110	0.052	
				0.030	0.186	0.342		
				0.059				
$\sum vi^+$	**5.006**	**4.906**	**4.918**	**0.806**	**1.142**	**1.181**	**0.960**	

Note. In the Na column, due to the partial occupation of the three sites, for each oxygen atom the first line corresponds to the electrostatic valencies received by the oxygen atoms from the cations taking account of the sodium population; the sum of the two lines corresponds to the valences received by the cations from the oxygen atoms.

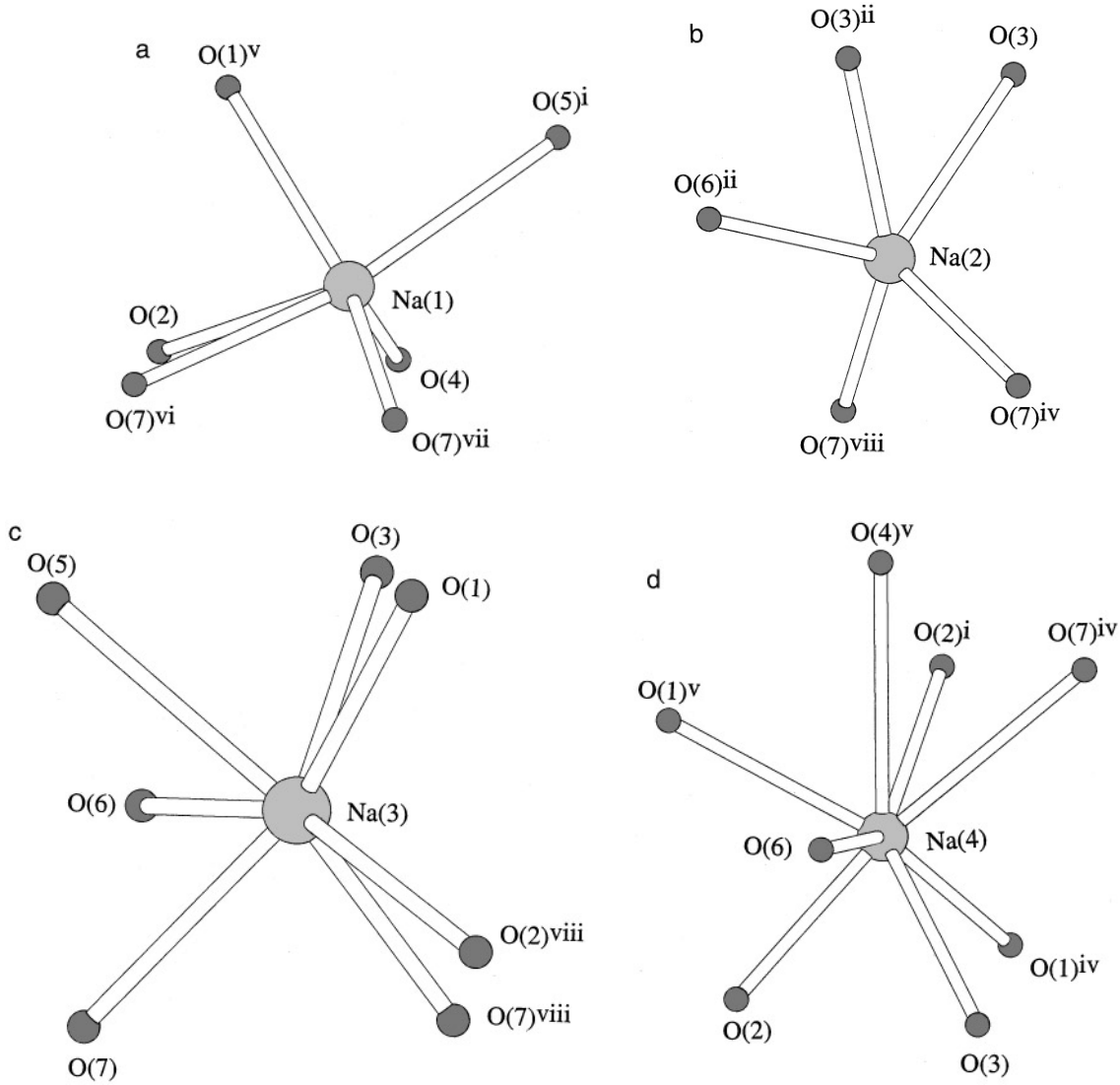

FIG. 7. The surrounding of Na^+ cations.

and that the thermal factors of these atoms are abnormally high, ranging from 3 to 7 $Å^2$ (Table 2).

The Na(1) sites, which exhibit the highest occupancy, are located at the intersection of the large [001] 10-sided tunnels and [10 $\bar{1}$] hexagonal tunnels. They are surrounded by eight oxygen atoms, with distances ranging from 2.38 to 2.88 Å (Table 3), forming a distorted trigonal prism with the six nearest neighbors (Fig. 7a).

The Na(2) cations located at the intersection of the [001] and [101] tunnels exhibit trigonal bipyramidal coordination (Fig. 7b), with Na–O distances ranging from 2.22 to 2.75 Å. Note that these sites are half-occupied (0.42) and that the thermal factor of Na(2) (4.5 $Å^2$) is larger than that for Na(1) despite its shorter Na–O distances.

The Na(3) cations are quite remarkable. They are located in the octagonal windows at the intersection of two large [001] tunnels and at the intersection of the [10 $\bar{1}$] tunnels. As a consequence they are linked to seven oxygen atoms, all located on the same side of a plane containing Na(3) (Fig. 7c), with Na–O distances ranging from 2.09 to 2.98 Å (Table 3). These cations which show a low occupancy at that site (0.25) exhibit an extremely high thermal factor (7 $Å^2$), suggesting a possible ionic mobility in agreement with the opened character of their polyhedron.

The Na(4) cations are the only ones that do not sit in the large [001] tunnels. Located at the intersection of the [101] and [10 $\bar{1}$] tunnels, they exhibit a bicapped trigonal prismatic coordination (Fig. 7d) with Na–O distances ranging from 2.37 to 3.00 Å (Table 3).

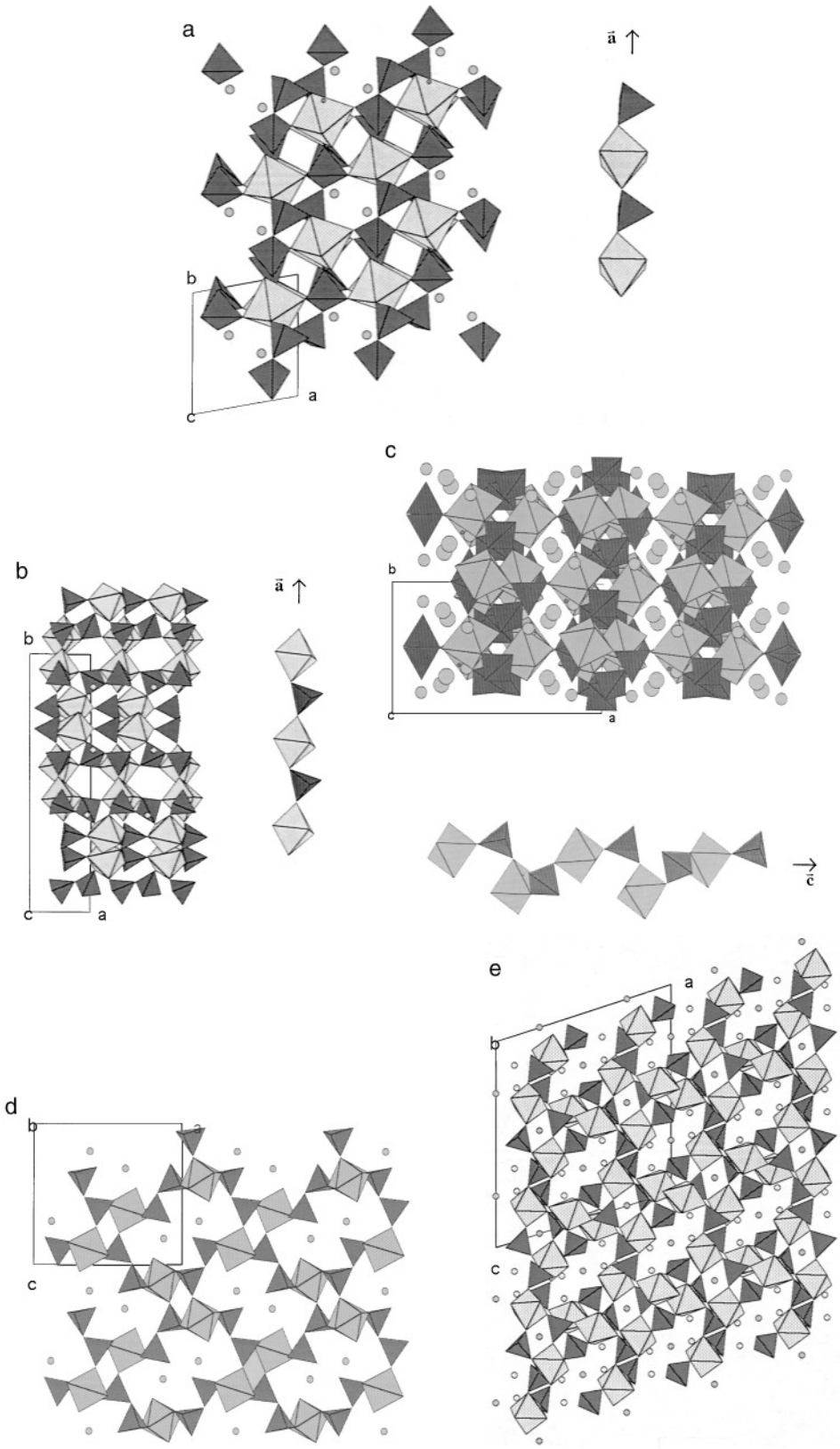

FIG. 8. (a) Projection of the structure of ε-$Na(MoO)_2(P_2O_7)(PO_4)$ along **c**. (b) Projection of the structure of ζ-$Na(MoO)_2(P_2O_7)(PO_4)$ along **c**. (c) Projection of the structure of $Na(MoO)_4(PO_4)_5$ along **c**. (d) Projection of the structure $NaMoOP_2O_7$ along **b**. (e) Projection of the $Li_2Na(MoO)_2(PO_4)_3$ along **b**.

Comparison with Other Sodium Molybdenyl Phosphates

The structures of the four other molybdenyl phosphates that have been synthesized to date are represented in Fig. 8. It appears clearly that each of these Mo(V) phosphates exhibits an original framework. Although they do not exhibit close relationships, these phosphates have a common feature: in all of them the MoO_6 octahedra are isolated, i.e., they share five apices with PO_4 tetrahedra, the sixth apex being free. Moreover three of them—ε–$Na(MoO)_2P_2O_7PO_4$ (Fig. 8a), ζ-$Na(MoO)_2P_2O_7PO_4$ (Fig. 8b), and $Na(MoO)_4(PO_4)_5$ (Fig. 8c)—are characterized like $Na_3(MoO)_2(PO_4)_3$ (Fig. 4) by existence of $[MoPO_8]_\infty$ chains in which one PO_4 tetrahedron alternates with one MoO_6 octahedron.

The most important structural property of these materials concerns the opened character of their structure which increases as the ratio Na : P increases. The phosphates ε-$Na(MoO)_2P_2O_7PO_4$ (Fig. 8a) and ζ-$Na(MoO)_2P_2O_7PO_4$ (Fig. 8b) which correspond to Na : P = 1/3 exhibit a cage structure, whereas $NaMoOP_2O_7$ (Fig. 8d) and $Na_3(MoO)_4(PO_4)_5$ (Fig. 8c) which exhibit Na : P molar ratios of 1/2 and 3/5 respectively are characterized by a tunnel structure. With a ratio Na : P = 1, the present monophosphate, $Na_3(MoO)_2(PO_4)_3$, exhibits so far the most opened real framework, due to the existence of intersecting tunnels and to their larger size. The monophosphate $Li_2Na(MoO)_2(PO_4)_3$ is difficult to compare owing to the simultaneous presence of lithium; nevertheless it is worth pointing out that this phase exhibits a tunnel structure (Fig. 8e), which can also be explained by the fact that the ratio Li + Na : P = 1 favors the opened character of the mixed "MoPO" framework.

Another interesting characteristic of these sodium molybdenyl phosphates concerns their ability to form interconnected cages or tunnels. This is the case of ε-$Na(MoO)_2P_2O_7PO_4$ and ζ-$Na(MoO)_2P_2O_7PO_4$ whose cages communicate through large windows and of $Na_3(MoO)_4(PO_4)_5$ and $Na_3(MoO)_2(PO_4)_3$ whose tunnels are also interconnected.

Among these phosphates, it is remarkable that $Na_3(MoO)_2(PO_4)_3$ exhibits the highest thermal factors for sodium up to 7 $Å^2$, compared to 4.5 $Å^2$ for $NaMoOP_2O_7$ and ε-$Na(MoO)_2P_2O_7PO_4$, and to values ranging from 1.5 to 3.3 $Å^2$ for the other sodium molybdenyl phosphates.

In conclusion the sodium molybdenyl phosphates form an interesting series of opened structures whose ionic conductivity will be studied. Among them, $Na_3(MoO)_2(PO_4)_3$ appears as most promising. Thus an effort is being made to produce it as a pure bulk material for physical studies.

REFERENCES

1. R. C. Haushalter and L. A. Mundi, *Chem. Mater*. **4,** 31 (1992).
2. G. Costentin, A. Leclaire, M.-M. Borel, A. Grandin, and B. Raveau, *Rev. Inorg. Chem.* **13,** 77 (1993).
3. A. Leclaire, T. Hoareau, M. M. Borel, A. Grandin, and B. Raveau, *J. Solid State Chem.* **114,** 543 (1995).
4. S. Ledain, A. Leclaire, M. M. Borel, J. Provost, and B. Raveau, *J. Solid State Chem.* **124,** 24 (1996).
5. A. Leclaire, M. M. Borel, A. Grandin, and B. Raveau, *J. Solid State Chem.* **89,** 10 (1990).
6. G. Costentin, M. M. Borel, A. Grandin, A. Leclaire, and B. Raveau, *J. Solid State Chem.* **89,** 31 (1990).
7. S. Ledain, A. Leclaire, M. M. Borel, and B. Raveau, *J. Solid State Chem.* **129,** 298 (1997).